

See discussions, stats, and author profiles for this publication at: <https://www.researchgate.net/publication/231666056>

Quantum–Mechanical Modeling of the Femtosecond Isomerization in Rhodopsin

ARTICLE *in* THE JOURNAL OF PHYSICAL CHEMISTRY B · JANUARY 2000

Impact Factor: 3.3 · DOI: 10.1021/jp992939g

CITATIONS

94

READS

15

2 AUTHORS:



Susanne Hahn

Primetals Technologies

12 PUBLICATIONS **235** CITATIONS

SEE PROFILE



Gerhard Stock

University of Freiburg

129 PUBLICATIONS **5,046** CITATIONS

SEE PROFILE

Quantum-Mechanical Modeling of the Femtosecond Isomerization in Rhodopsin

Susanne Hahn and Gerhard Stock*

Faculty of Physics, University of Freiburg, D-79104 Freiburg, Germany

Received: August 19, 1999; In Final Form: November 2, 1999

The photoisomerization of retinal in rhodopsin is modeled by a vibronically coupled electronic two-state system, taking into account a collective reaction coordinate and the ethylenic stretch mode. The model qualitatively reproduces all available spectroscopic information on rhodopsin and accounts for its high reaction efficiency. Quantum simulations of femtosecond time-resolved experiments suggest that the prominent 60 cm^{-1} oscillations observed in experiments are due to nonadiabatic wave packet motion along the reaction coordinate. This indicates that the protein is capable of providing an almost friction-free environment for retinal up to ≈ 2 ps, thereby catalyzing the photoreaction.

The first step in vision, the photoinduced 11-*cis* \rightarrow all- *trans* isomerization of retinal in rhodopsin, is one of the best-studied photoreactions in proteins.^{1,2} Femtosecond time-resolved experiments on rhodopsin have revealed that the photoproduct is formed with high efficiency and within only 200 fs.³ Furthermore, time-dependent oscillations in the absorption band of the photoproducts indicate that the first step in vision may be a vibrationally coherent process.⁴ Since none of the intriguing features of rhodopsin (high reaction speed and efficiency as well as vibrational coherence) are monitored for retinal in solution,⁵ these findings suggest that the protein represents a unique and highly optimized environment for the retinal chromophore. The observation of coherent femtosecond dynamics in a variety of photobiological systems moreover indicates that vibrational coherence may play a fundamental role in the efficient conversion of light into energy.⁶

Adopting a time-dependent view, a photochemical reaction can be rationalized in terms of a photoinduced vibrational wave packet evolving on an adiabatic potential-energy surface (PES), thereby defining a reaction path of the molecule from the reactants to the photoproduct (see Figure 1). In the case of femtosecond photochemistry,⁷ moreover, quantum-chemical studies have established that many ultrafast photoreactions are intimately connected with the internal conversion of the molecule via a so-called *conical intersection* of PESs.^{8,9} A microscopic understanding of these reactions therefore requires to extend the Born–Oppenheimer picture of nuclear motion on a single adiabatic PES to the concept of *nonadiabatic* dynamics on several vibronically coupled PESs. While classical trajectory simulations are a well-established tool to account for molecular equilibrium properties, the dynamical description of photoinduced excited-state processes in complex systems is still in its very beginnings.^{9–15}

Two features of conical intersections support the occurrence of coherent femtosecond photoreactions: (i) Since the non-adiabatic couplings become singular at surface crossings, the corresponding electronic relaxation is a very fast and efficient process that is expected to completely dominate the dynamics on a femtosecond time scale. (ii) The reaction is mode-selective since typically only specific vibronically active vibrational modes give rise to an intersection of PESs.⁸ This suggests that

the femtosecond response of complex molecular systems may be described by a highly reduced model which solely includes the electronic states and vibrational modes directly involved in the dominant internal-conversion process.

Here, we report on first attempts to employ this approach to the quantum-mechanical modeling of the ultrafast isomerization in rhodopsin. As a *minimal model* of this process, we adopt an electronic two-state system comprising a reaction coordinate ϕ leading from the *cis* to the *trans* conformation and a single vibronically active coordinate x_C that may couple the two electronic states. Exact time-dependent quantum calculations have shown that this type of model is suitable to reveal basic features of isomerization, internal conversion, and vibrational relaxation.^{9,16} To account for the excited-state absorption exhibited by rhodopsin, we have furthermore included an additional higher-lying electronic state that does not participate in the photochemical reaction under consideration.

Adopting a diabatic representation of the electronic ground state S_0 and the first excited state S_1 , the molecular Hamiltonian is given as the sum of the (diagonal) kinetic energy T and the diabatic potential matrix¹⁷

$$H = T\mathbf{1} + \begin{pmatrix} V_0 & V_{01} \\ V_{10} & V_1 \end{pmatrix}$$

whereby $V_k = V_k^R(\phi) + V_k^C(x_C)$ and $V_{kk'} = V_{kk'}(x_C)$.¹⁸ The two nuclear degrees of freedom ϕ and x_C of the model are assumed to be *effective* coordinates, each representing different aspects of the photoreaction: The reaction coordinate accounts for the energy relations of the reaction (see below), while the coordinate x_C collectively represents all vibrations q_j that couple to the electronic S_0 – S_1 transition (i.e., with nonzero gradients $\partial(V_1 - V_0)/\partial q_j$ and $\partial V_{01}/\partial q_j$).

The motivation to use a collective vibronic mode x_C stems from simple valence-bond model considerations¹⁹ as well as from recent *ab initio* molecular-dynamics simulations.^{12–14} These studies indicate that the initial optical response of polyconjugated molecules is characterized by a delocalized stretching motion of the polyene chain, whereby single and double bonds interchange. This conclusion is in agreement with the dominant vibronic activity of the ethylenic stretch modes at $\approx 1550 \text{ cm}^{-1}$ as observed in ground- and excited-state

* Corresponding author. E-mail: stock@physik.uni-freiburg.de

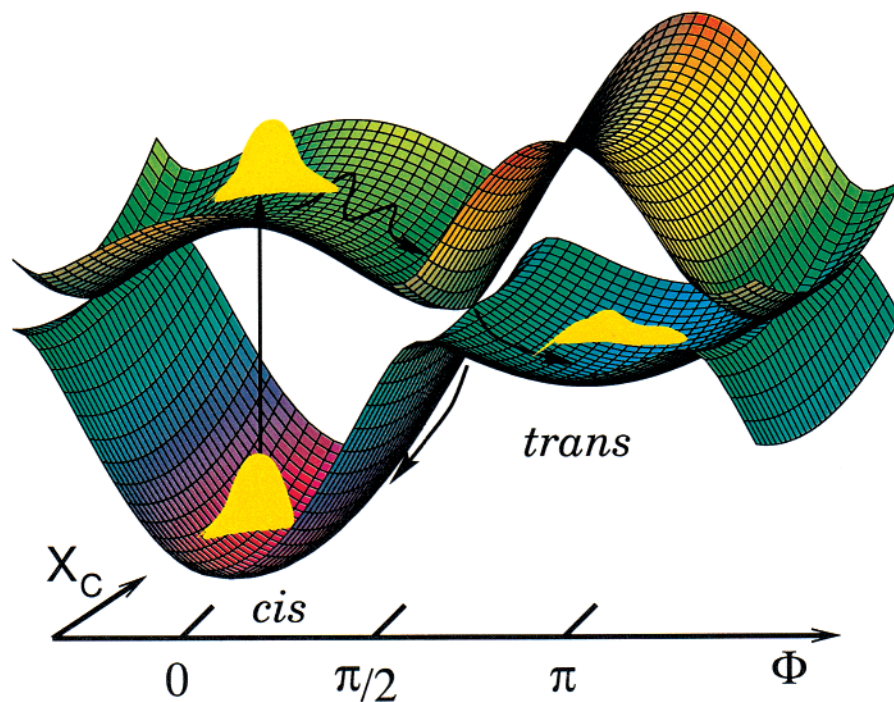


Figure 1. Adiabatic potential-energy surfaces of the two-state two-mode model of the cis–trans isomerization in rhodopsin. Upon vertical excitation by the pump pulse, a vibrational wave packet is prepared which subsequently bifurcates at the conical intersections located at $\phi = \pm\pi/2$. Employing time-delayed probe pulses that are resonant with the energy gap of the cis and trans configuration, respectively, the dynamics of the photoreaction can be monitored in real time.

resonance-Raman experiments.^{20,21} To account for these findings, a vibrational mode of this frequency is included, which is described within the harmonic approximation.¹⁸ For the reaction-coordinate potentials we choose the ansatz:¹⁶

$$V_0^R(\phi) = 1/2W_0(1 - \cos \phi)$$

$$V_1^R(\phi) = E_1 - 1/2W_1(1 - \cos \phi)$$

The three parameters E_1 , W_0 , W_1 are determined by (i) taking into account the energy storage $\Delta E = E_1 - W_1$ of the photoreaction and (ii) requiring that the electronic S_0 – S_1 gap pertaining to the cis and trans conformation match the center frequency of the absorption bands of the two isomers, respectively. The effective mass m pertaining to the motion along ϕ can be determined (i) from experimental Raman data revealing the ground-state frequency $\omega_R = \sqrt{W_0/2m}$ of modes that are believed to reflect isomerization, (ii) by requiring that isomerization takes place within 200 fs as observed in time-resolved experiments. Interestingly, the latter condition corresponds to $\omega_R = 238 \text{ cm}^{-1}$, which is in good agreement with the main low-frequency Raman emission observed for rhodopsin at $\approx 250 \text{ cm}^{-1}$.²⁰ It should be stressed that the thus defined reaction coordinate does not necessarily correspond to a specific internal coordinate of retinal (e.g., the $C_{11}=C_{12}$ torsional mode) but collectively accounts for the energy relations of the reaction. The effect of the protein environment is thereby included in the parameters m , E_1 , W_0 , and W_1 of the model.

Employing this two-state two-mode model, we have performed detailed numerical simulations of the photoinduced dynamics and various optical spectra.²² Hereby, we are able to qualitatively reproduce all available spectroscopic information on rhodopsin. The most challenging application of the model is the explanation of the transient absorption experiments on rhodopsin,^{3,4} which is the subject of the remainder of the paper.

Since the dynamical methodology is numerically exact, all results and conclusions are a direct consequence of the model introduced above.

In the experiment of Wang et al.,⁴ rhodopsin was excited by a 35 fs pump pulse at 500 nm and transient changes in absorption were measured from 450 to 640 nm by employing 10 fs probe pulses. Figure 2 shows the theoretical simulation of this experiment as obtained for the proposed model of the cis–trans isomerization in rhodopsin.²² In agreement with experiments, the time- and frequency-resolved spectrum consists of two spectral bands centered at 500 and 570 nm. For early times ($t \approx 0$), the signal at 500 nm is dominated by a strong (positive-going) excited-state absorption feature at 500 nm which changes into a (negative-going) bleach signal after ≈ 50 fs. For larger times ground-state bleach, stimulated emission, as well as excited-state absorption contribute to the 500 nm band, which therefore mainly reflects the dynamics of the cis reactant. The signal at 570 nm, on the other hand, reaches its first maximum at ≈ 200 fs, thus reflecting the onset of the trans photoproduct absorbance. Both parts of the spectrum are seen to exhibit a pronounced beating with a period of ≈ 500 fs corresponding to a frequency of $\approx 60 \text{ cm}^{-1}$.

As a comparison of experiment and theory, Figure 3 shows cuts of the transient absorption spectrum at (a) 500 nm and (b) 570 nm. The simulations clearly reproduce the 60 cm^{-1} oscillations, which are seen to be shifted in phase by 180° for the two signals. This beating is superimposed by high-frequent oscillations which are qualitatively matched by the calculation, e.g., the simulation for 570 nm reproduces the two intermediate maxima at $t \approx 400$ and 1000 fs. The deviations between experiment and theory observed for $t \gtrsim 1500$ fs indicate that at these times additional degrees of freedom not considered in the model need to be included. To explain the femtosecond spectra in terms of the isomerization dynamics of the molecular model employed, Figure 3c shows the time-dependent probability of

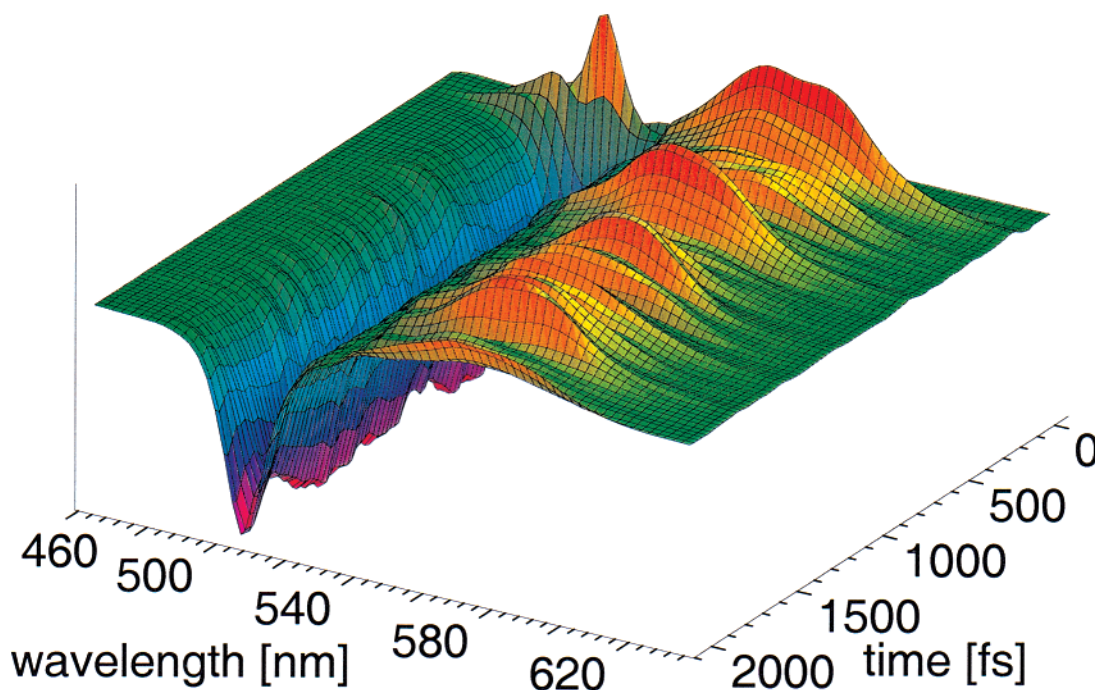


Figure 2. Simulated transient absorption spectrum as obtained for the proposed model of the cis–trans isomerization in rhodopsin. The spectral band at 500 nm reflects the dynamics of the reactants, while the 570 nm band reflects the absorbance of the photoproducts.

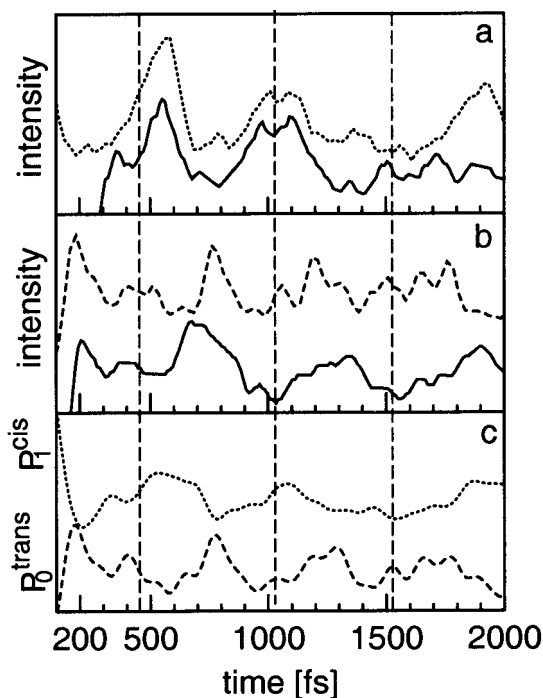


Figure 3. Comparison of calculated and experimental (full lines, adopted from ref 4) transient absorbance of rhodopsin at (a) 500 nm and (b) 570 nm. An exponential component has been subtracted from the 500 nm signals in order to facilitate the representation of the oscillations. (c) Time-dependent probability of the system to be in the cis configuration of the upper adiabatic electronic state (dotted line) and in the trans configuration of the lower adiabatic state (dashed line), respectively. The vertical dashed lines mark the prominent beating with a period of ≈ 500 fs.

the system to be in the cis configuration of the upper adiabatic electronic state [$P_1^{\text{cis}}(t)$] and in the trans configuration of the lower adiabatic state [$P_0^{\text{trans}}(t)$], respectively. The similarity between the intramolecular quantities and the simulated spectra clearly suggests that the 500 and 570 nm signals monitor the

dynamics of the reactants and photoproducts, respectively. Furthermore, the simulation predicts a reaction quantum yield of ≈ 0.63 ,²³ which is in good agreement with the experimental value of 0.67.

We are now in a position to discuss the results of the simulations in terms of time-dependent wave packet motion on coupled PESs (see Figure 1). At time $t = 0$ the pump pulse prepares a wave packet on the upper PES in the cis configuration ($\phi \approx 0$). Following the gradient of the PES, the wave packet bifurcates at the conical intersections at ($\phi \approx \pm\pi/2$). The major part of it reaches the S_0 trans configuration ($\phi \approx \pi$) at $t = 200$ fs, which results in the first peak of $P_0^{\text{trans}}(t)$ as well as of the photoproduct-absorbance signal at 570 nm. Despite further bifurcations at $\phi \approx k\pi/2$ ($k = 1, 2, \dots$), a fraction of the wave packet manages to climb back up to the S_1 cis conformation, thus causing maxima at $t = 600, 1100, 1500$, and 1900 fs of $P_1^{\text{cis}}(t)$. Corresponding peaks are observed in the 500 nm signal, which in the Franck–Condon region is dominated by the excited-state absorption. On the other hand, the prominent peaks of $P_0^{\text{trans}}(t)$ as well as of the photoproduct-absorbance signal at $t \approx 200, 700, 1300$, and 1800 fs clearly indicate that the wave packet is in the S_0 trans configuration. The 60 cm^{-1} oscillations of the transient absorption signal can therefore be attributed to quasiperiodic motion along the *diabatic* reaction potential curve V_1^R . Hereby the traveling wave packet causes photoproduct-absorbance in the S_0 trans configuration and an excited-state absorption from the S_1 cis configuration that is shifted in phase by 180° .

Assuming that the features seen in experiment and simulation are of the same origin, the analysis of the quantum calculations is found to lead to a more complex interpretation than the original explanation, which attributed the 60 cm^{-1} beating to oscillations in the S_0 trans photoproduct.⁴ Given the experimental data alone, the latter interpretation clearly appears as the most likely physical picture. The model calculations are also in accordance with experimental findings, but beyond that, they allow us to reproduce and explain a great deal of the experimental data on rhodopsin. For example, the model identifies

the onset of the 570 nm absorbance within 200 fs, the 60 cm^{-1} beating, as well as the prominent 250 cm^{-1} Raman emission as interrelated effects due to the same reaction coordinate. Furthermore, the theory reproduces the high-frequency (170 and 240 cm^{-1}) components of the transient signals, which are a consequence of the bifurcations of the wave packet. It should be stressed that the vibrational frequencies thus established have not been assumed beforehand, but are merely a consequence of the (independently determined) parameters of the reaction potentials.

Taking the numerical results as evidence that an effective two-state two-mode model may indeed account for essential features of the femtosecond response of biophysical systems, the following questions arise: (i) What is the microscopic nature of the collective modes introduced, and (ii) what is the effect of the protein environment on the initial photoreaction? While the first question probably can be answered only through quantum-chemical investigations, the second question may shed some light on the connection between coherent femtosecond dynamics, high reaction efficiency, and the effects of the protein environment. In the case of small molecules in the gas phase, the enhancement of femtosecond photoreactions by coherent vibrational motion is well established.⁷ As a well-studied example consider the photoinduced predissociation of sodium iodine which is promoted by the vibrational motion of NaI. In the case of larger molecules in solution, vibrationally promoted photophysical processes such as photoinduced electron-transfer have been observed on a sub-100 fs time scale.²⁴ Considering photobiological systems, however, the fastest time scale of chemically reactive nuclear motion is expected to be on the order of several hundred femtoseconds, thus hampering coherent vibrational motion under solution conditions. The observation of the 60 cm^{-1} oscillations in rhodopsin thus indicate that the protein is capable of providing an almost friction-free environment for retinal up to ≈ 2 ps, thereby catalyzing the photoreaction. Moreover, it is this effect of the protein environment that makes it feasible to describe a photobiological reaction in terms of a highly reduced model.

Several conclusions may be drawn. First, it is interesting to note that an effective two-state two-mode model is able to qualitatively reproduce the femtosecond response of a complex biophysical system such as rhodopsin. In particular, the model is able to account for the high quantum yield of the isomerization, thus indicating that the high reaction efficiency observed for rhodopsin is indeed facilitated by the femtosecond dynamics of retinal. Furthermore, the proposed quantum model suggests that the 60 cm^{-1} oscillations in the measured transient absorbance is caused by nonadiabatic wave packet motion on coupled PESs. Thus, presumably independent experimental findings on rhodopsin such as the onset of the 570 nm absorbance within 200 fs, the 60 cm^{-1} beating, as well as the prominent 250 cm^{-1} Raman emission can be consistently explained as interrelated effects due to the same reaction coordinate. In summary, explicit quantum simulations of femtosecond experiments on rhodopsin have shown that the primary process of vision can be rationalized in terms of a two-dimensional wave packet motion on coupled PESs, thereby demonstrating the primary role of nonadiabatic interactions in femtosecond photobiological processes.

Acknowledgment. We thank W. Domcke, P. Hamm, F. Siebert, and J. Wachtveitl for stimulating discussions. Financial support by the Deutsche Forschungsgemeinschaft and the Fonds der Chemischen Industrie is gratefully acknowledged.

References and Notes

- (1) Birge, R. R. *Biochim. Biophys. Acta* **1990**, *1016*, 293.
- (2) Koechendoerfer, G. G.; Mathies, R. A. *Isr. J. Chem.* **1995**, *35*, 211.
- (3) Peteanu, L. A.; Schoenlein, R. W.; Mathies, R. A.; Shank, C. V. *Proc. Natl. Acad. Sci. U.S.A.* **1993**, *90*, 11762. Chosrowjan, H.; Mataga, N.; Shibata, Y.; Tachibana, S.; Kandori, H.; Shichida, Y.; Okada, T.; Kouyama, T. *J. Am. Chem. Soc.* **1998**, *120*, 9706. Haran, G.; Morlino, E. A.; Matthes, J.; Callender, R. H.; Hochstrasser, R. M. *J. Phys. Chem. A* **1999**, *103*, 2202.
- (4) Wang, Q.; Schoenlein, R. W.; Peteanu, L. A.; Mathies, R. A.; Shank, C. V. *Science* **1994**, *266*, 422.
- (5) Logunov, S. L.; Song, L.; El-Sayed, M. A. *J. Phys. Chem.* **1996**, *100*, 18586.
- (6) Coherence in Chemical Dynamics. Ruhman, S.; Scherer, N., Eds.; *Chem. Phys.* **1998**, 233.
- (7) Zewail, A. H. *Femtochemistry—Ultrafast Dynamics of the Chemical Bond*; World Scientific: Singapore, 1994.
- (8) Michl, J.; Bonačić-Koutecký, V. *Electronic Aspects of Organic Photochemistry*; Wiley: New York, 1990; Bernardi, F.; Olivucci, M.; Robb, M. A. *Chem. Soc. Rev.* **1996**, *25*, 321; Köppel, H.; Domcke, W. *Encyclopedia of Computational Chemistry*; Schleyer, P. v. R., Ed.; Wiley: New York, 1998.
- (9) Domcke, W.; Stock, G. *Adv. Chem. Phys.* **1997**, *100*, 1.
- (10) Warshel, A. *Nature (London)* **1976**, *260*, 679; Warshel, A.; Chu, Z. T.; Hwang, J.-K. *Chem. Phys.* **1991**, *158*, 303.
- (11) Schulten, K.; Tavan, P. *Nature (London)* **1978**, *272*, 85; Ben-Nun, M.; Molnar, F.; Lu, H.; Philips, J. C.; Martinez, T. J.; Schulten, K. *Faraday Discuss.* **1998**, *110*, 447.
- (12) Vreven, T.; Bernardi, F.; Garavelli, M.; Olivucci, M.; Robb, M. A.; Schlegel, H. B. *J. Am. Chem. Soc.* **1997**, *119*, 12687; Garavelli, M.; Vreven, T.; Celani, P.; Bernard, F.; Robb, M. A.; Olivucci, M. *J. Am. Chem. Soc.* **1998**, *120*, 1285.
- (13) La Penna, G.; Buda, F.; Bifone, A.; de Groot, H. J. M. *Chem. Phys. Lett.* **1998**, *294*, 447.
- (14) Tsiper, E. V.; Chernyak, V.; Tretiak, S.; Mukamel, S. *J. Chem. Phys.* **1999**, *110*, 8328.
- (15) Berweger, C. D.; Müller-Plathe, F.; van Gunsteren, W. F. *J. Chem. Phys.* **1999**, *108*, 8773.
- (16) Seidner, L.; Domcke, W. *Chem. Phys.* **1994**, *186*, 27.
- (17) Diagonalizing the *diabatic* potential matrix, the *adiabatic* PESs shown in Figure 1 are obtained.
- (18) The matrix elements of the Hamiltonian are: $T = -1/2\omega \partial^2/\partial x_C^2 - 1/2m^{-1} \partial^2/\partial \phi^2$, $V_k^C = 1/2\omega x_C^2 + \kappa_k x_C$, $V_{01} = V_{10} = \lambda x_C$. The parameters of the model are in [eV]: $m^{-1} = 4.84 \times 10^{-4}$, $E_1 = 2.48$, $W_0 = 3.6$, $W_1 = 1.09$, $\omega = 0.19$, $\kappa_0 = 0$, $\kappa_1 = 0.1$, $\lambda = 0.19$. The higher-lying electronic state is characterized by $V_{02} = V_{12} = 0$, $E_2 = 2.43$, $W_2 = W_0$, $\kappa_2 = \kappa_0$.
- (19) Lu, D.; Chen, G.; Perry, J. W.; Goddard, W. A., III. *J. Am. Chem. Soc.* **1994**, *116*, 10679. Del Zoppo, M.; Tommasini, M.; Castiglioni, C.; Zerbi, G. *Chem. Phys. Lett.* **1998**, *287*, 100.
- (20) Lin, S. W.; Groesbeck, M.; van der Hoef, I.; Verdegem, P.; Lugtenburg, J.; Mathies, R. A. *J. Phys. Chem. B* **1998**, *102*, 2787.
- (21) Song, L.; El-Sayed, M. A. *J. Am. Chem. Soc.* **1998**, *120*, 8889.
- (22) Employing a nonperturbative methodology,⁹ the time-dependent Schrödinger equation for the molecular Hamiltonian and the field-matter interaction has been solved numerically exactly. To this end, the state vector has been expanded in a direct-product basis constructed from the three diabatic electronic states, 150 free-rotor states for the reaction coordinate, and 24 harmonic-oscillator states for the coupling coordinate. This results in a system of 10 800 coupled first-order differential equations which are driven by the electric field of the laser pulses. The nonperturbative method allows for a direct simulation of an arbitrary nonlinear spectroscopic experiment, including effects of high intensities and overlapping pump and probe fields. Furthermore, it allows us to discriminate the individual spectroscopic processes such as ground-state bleach, stimulated emission, excited-state absorption, and product absorption.
- (23) Assuming that for large times the electronic excited state is completely decayed into the adiabatic ground state, the quantum yield of the *cis*-*trans* reaction may be defined as $P_0^{\text{trans}}(\infty)/[P_0^{\text{cis}}(\infty) + P_0^{\text{trans}}(\infty)]$.
- (24) See, e.g., Wolfseider B. et al., in ref 6, p 323.